Published in final edited form as:
*Bioorg Med Chem Lett*. 2012 January 1; 22(1): 683–688. doi:10.1016/j.bmcl.2011.10.054.

# Hoiamide D, a marine cyanobacteria-derived inhibitor of p53/MDM2 interaction

**Karla L. Malloy**[a,b,†], **Hyukjae Choi**[a,b,†], **Catherine Fiorilla**[c], **Fred A. Valeriote**[d], **Teatulohi Matainaho**[e], and **William H. Gerwick**[a,b,*]

[a]Center for Marine Biotechnology and Biomedicine, Scripps Institution of Oceanography, University of California at San Diego, La Jolla, California 92093

[b]Skaggs School of Pharmacy and Pharmaceutical Sciences, University of California at San Diego, La Jolla, California 92093

[c]Novartis Institutes of Biomedical Research, Cambridge, Massachusetts 02139

[d]Henry Ford Health System, Department of Internal Medicine, Josephine Ford Cancer Center, Detroit, MI 48202

[e]Discipline of Pharmacology, School of Medicine and Health Sciences, University of Papua New Guinea, National Capital District, Papua New Guinea

## Abstract

Bioassay-guided fractionation of two cyanobacterial extracts from Papua New Guinea has yielded hoiamide D in both its carboxylic acid and conjugate base forms. Hoiamide D is a polyketide synthase (PKS)/non-ribosomal peptide synthetase (NRPS)-derived natural product that features two consecutive thiazolines and a thiazole, as well as a modified isoleucine residue. Hoiamide D displayed inhibitory activity against p53/MDM2 interaction ($EC_{50}$= 4.5 μM), an attractive target for anticancer drug development.

### Keywords

marine cyanobacteria; natural products; lipopeptide; anticancer; spectroscopy

The protein p53 is a well characterized tumor suppressor that acts as a transcription factor to regulate cell cycle dynamics, apoptosis, and DNA repair.[1] It is encoded by the gene TP53 that is inactivated in nearly 60% of all human malignancies.[2] Structurally, p53 harbors an $NH_2$ terminal transactivation domain, a DNA binding domain in the center, and a C-terminal locus for regulatory function and tetramerization.[3] Its function is regulated either by mutation or deletion of the parent gene or through regulatory feedback by MDM2. MDM2, a murine ubiquitin ligase, negatively regulates p53 function by a variety of mechanisms, including degradation through proteosomal association and ubiquitylation. MDM2 also



*To whom correspondence should be addressed. Tel: (858) 534-0578. Fax: (858) 534-0529. wgerwick@ucsd.edu.
†These authors contributed equally



**Supplementary Data**
Supplementary data associated with this article can be found, in the online version, at.

facilitates nuclear export with its export signal and binds to p53's transactivation domain, thereby repressing transcriptional activity.[3,4] Recent studies have also shown MDM2 to interact, albeit more weakly, with the C-terminal and core domains of p53.[5] In theory, disruption of any of these regulatory functions by MDM2 is a viable strategy to reactivate p53, especially through inhibition of the p53/MDM2 binding interaction.

Based on site directed mutagenesis, the essential amino acids of the p53 N-terminal binding domain that constitute the majority of the p53/MDM2 interaction and binding energy are $Phe^{19}$-$Trp^{23}$-$Leu^{26}$, with the three terminal atoms of the phenyl ring, the indole nitrogen of tryptophan (Trp), and the isopropyl group of leucine (Leu) serving as the pertinent pharmacophore.[3,6] Thus, the p53/MDM2 interaction is largely hydrophobic, and the binding interface of the two proteins is also quite small, making small, peptidic or non-peptidic molecular mimics of the p53 binding site good candidates for inhibitors of p53/MDM2 interaction.[3,6] This hydrophobic binding domain has been exploited to rationally design synthetic p53/MDM2 inhibitors with excellent affinity. Three major classes of synthetic p53/MDM2 inhibitors, the nutlins, spiro-oxindoles, and benzodiazepinediones, have taken advantage of the $Phe^{19}$-$Trp^{23}$-$Leu^{26}$ binding core to displace p53 and bind MDM2 with much greater affinity and in vitro potency. However, maintaining in vivo potency has been problematic for many of these inhibitors due to their poor pharmacokinetic profiles.[7,8]

Marine cyanobacteria are one of Nature's most ancient organisms and offer a plethora of bioactive secondary metabolites, many of which are active against validated targets of human disease. Of the 678 marine cyanobacterial natural products reported in the literature, the majority is polyketide synthase-non-ribosomal peptide synthetase derived.[9] There is a predominance of nonpolar amino acids in cyanobacterial peptide-derived compounds, and leucine and phenylalanine, two essential amino acids of the p53 binding pocket, are relatively common constituents in these peptidic compounds. Approximately half of all amino acids utilized in cyanobacterial natural products are modified with the most frequent modifications including *N*-methylation, *N'*-*N'*-dimethylation, ketide extension, and halogenation to a lesser extent.[9] Thus, many features of marine cyanobacterial compounds, including their molecular weight distribution (median 604 Da), lipophilicity, and chemical diversity, lend themselves to favorable bioactivity and medicinal chemistry profiles, particularly as it pertains to p53/MDM2 inhibition. Herein, we describe hoiamide D (**1**), a peptide-derived p53/MDM2 inhibitor, isolated in both its acid and carboxylate forms, from two separate collections of the Papua New Guinea cyanobacterium *Symploca* sp. Hoiamide D displays promising inhibitory activity towards p53/MDM2 interaction ($EC_{50}$= 4.5 μM).

Samples of the spongy, purple cyanobacterium *Symploca* sp. were collected by SCUBA near Kape Point, Papua New Guinea in 2006. The collection was extracted with $CH_2Cl_2$:MeOH (2:1) to yield a crude extract (1.37 g) that was further processed using normal phase silica vacuum liquid chromatography to generate nine subfractions (A-I).[10] The ninth and most polar fraction (I) displayed inhibitory activity in the p53/MDM2 assay and was further purified using RP C18 solid phase extraction to yield an additional four relatively pure subfractions. The most polar subfraction (>95% pure) contained the new natural product, hoiamide D (23.6 mg), and harbored the greatest inhibitory activity ($EC_{50}$= 4.5 μM).

The HRESIMS measurement of hoiamide D (**1**), $[M+H]^+$ *m/z* 743.3535, established its formula as $C_{35}H_{58}N_4O_7S_3$ with an isotopic pattern consistent with the presence of three sulfur atoms.[11] The IR spectrum of **1** displayed an absorption band at 3381 $cm^{-1}$, indicating the presence of a hydroxy group while the $^1H$ NMR spectrum revealed two distinctive low-field shifts, a sharp singlet at $\delta_H$ 8.22 ($\delta_C$ 122.6) and a doublet at $\delta_H$ 6.85 that were indicative of a substituted alkene and an amide, respectively. A singlet at $\delta_H$ 3.23 ($\delta_C$ 56.2) revealed the presence of an O-Me substituent, and two sharp high-field singlets between

1.4-1.6 ppm were suggestive of deshielded methyl groups. 2D COSY, HSQC, TOCSY, and HMBC experiments were subsequently used to elucidate three partial structures (A-C) with key HMBC correlations used to provide attachment points and complete the planar structure, as described below.

TOCSY data afforded a two-spin system for substructure (A) with one spin system consisting of H-2/H-3/H-9 and the other spin system consisting of H4-H8. A COSY correlation between H-4 and the amide proton at $\delta_H$ 6.85, as well as HMBC correlations between H-4/C-5, $H_3$-8/C-5, H-6a/C-3, and $H_3$-7/C-6, supported construction of a modified isoleucine with a hydroxy at C-3 ($\delta_C$ 71.8, $\delta_H$ 3.51). The C-3 methine was coupled to the C-2 methine via a COSY correlation and through to the C-1 carbonyl with a 3-bond HMBC correlation. A methyl ($\delta_C$ 13.8, $\delta_H$ 0.85) was then assigned to C-2 via H-2/C-9 and $H_3$-9/C-1 HMBC correlations, thus completing the planar substructure (A) or 4-amino-3-hydroxy-2,5-dimethylheptanoic acid (Ahdhe), a structural feature characteristic of the hoiamide class (Figure 2).

Substructure (B) featured two consecutively coupled α-methyl thiazoline rings and a thiazole. Preliminary data analysis suggested that two methylenes with chemical shifts $\delta_H$ 3.59/3.13 ($\delta_C$ 40.9); $\delta_H$ 3.74/3.76 ($\delta_C$ 42.2) were adjacent to heteroatoms, and a low-field singlet at $\delta_H$ 8.21 ($\delta_C$ 122.6) implied the presence an olefinic proton of a heterocycle. Atom counting and the presence of three deshielded quaternary carbons C-14/18/21 ($\delta_C$ 177.7, 162.5, 169.9) also suggested that these $sp^2$ carbons were proximate to a nitrogen and a sulfur atom in each ring. HMBC correlations were then used to construct the rings of the triheterocyclic system, as follows. A correlation between the C-12 methylene ($\delta_C$ 40.9) and the deshielded $sp^2$ C-14 ($\delta_C$ 177.7) permitted assignment of C-12 adjacent to the sulfur atom with C-14 placed between the sulfur and nitrogen atoms. An additional HMBC correlation between $H_2$-12 and the relatively shielded quaternary carbon at C-11 ($\delta_C$ 84.4) necessitated placement of C-11 adjacent to a nitrogen atom and between the C-12 methylene and the carbonyl at C-10. Further HMBC correlations between $H_3$-13/C-10/11/12 permitted assignment of an α-methyl group on C-11 of the thiazoline ring. In a similar fashion, the second thiazoline ring was constructed with HMBC correlations between the C-16 methylene, the deshielded $sp^2$ C-18 ($\delta_C$ 162.5), and the relatively shielded quaternary carbon at C-15 ($\delta_{C15}$ 83.6). Additional correlations between $H_3$-17/C-15/16 permitted assignment of an α-methyl group on C-15 of the second thiazoline ring as well. The third ring was constructed with HMBC correlations from a low-field olefinic proton at $\delta_H$ 8.21 ($\delta_C$ 122.6) to two $sp^2$ quaternary carbons at C-19/21which implied the presence of a thiazole ring and satisfied the remaining degrees of unsaturation for the molecule. Further correlations between H-16a/16b/C-14 and H-20/C-18 demonstrated the consecutive nature of the triheterocyclic ring system to complete substructure (B).

Substructure (C) consisted of an extended 10-carbon chain with two hydroxy and three methyl groups, and a methoxy substituent. COSY correlations were used to consecutively assign the H-22 methylene with three methines H-23/24/25. An additional COSY correlation was used to assign a methyl group at C-24 ($\delta_{H24}$ 2.08), and an HMBC correlation between C-23 and the H-35 *O*-methyl allowed placement of the *O*-methyl at this position. COSY correlations were also used to assign the H-26/27/28 methines and two methyl groups at C-26 ($\delta_{H26}$1.52) and C-28 ($\delta_{H28}$1.54), respectively. A 3-bond HMBC correlation between $H_3$-33 and C-25 allowed connection of C25/C26. Further COSY correlations were then used to place the H-29 and H-30 methylenes adjacent to the terminal C-31 methyl group. HMBC correlations between the C-28 methine and both H-29a/H-29b protons then permitted connection of C-28/29. Accounting of the remaining atoms and chemical shift reasoning allowed hydroxy groups to be placed at C-25 ($\delta_C$ 69.4) and C-27 ($\delta_C$ 72.7) to complete substructure (C).

Finally, a key HMBC correlation between the C-10 carbonyl and the H-13 α-methyl connected substructure (A) with substructure (B), and HMBC correlations between C21 and H22/H23 permitted connection of substructure (B) to (C), thereby completing the proposed planar structure of **1** (Figure 1).

Colon cancer selectivity-guided fractionation of a second collection of mat-forming *Symploca* sp. obtained near Kolaio island, Papua New Guinea in 2003 yielded **2** with a HRESI $[M+H]^+$ *m/z* 743.3535 mass identical to **1**.[12,13] Independent structure elucidation of **2** led to the same planar structure of **1**. However, subsequent analysis of spectroscopic and analytical data revealed subtle differences between **1** and **2** that suggested the possibility of either different stereoisomers, different ionic states, or some other small difference. First, $\Delta\delta_C$ values of C-1-C-4 and C-6 and $\Delta\delta_H$ values of H-2 and H-3 are significant between **1** and **2** with the greatest $\Delta\delta_C$ nearly 3 ppm at C-1 (Figure 3a). One hypothesis accounting for the carbon shift difference was the possibility of different stereoisomers. However, coupling constant analysis did not reveal significant differences between **1** and **2**. Another possibility to account for the carbon shift disparity was a difference in ionic states. The more deshielded carbon of **1** ($\delta_C$ 179.5) suggests **1** may be the conjugate base of **2**. Second, **1** and **2** were obtained by different chromatographic conditions; **1** was isolated under neutral conditions while **2** was purified with an acidified buffer. A LC-ESI-MS co-injection experiment, with simultaneous elution of **1** and **2** in various chromatographic conditions, also provided supporting evidence of constitutional equivalence but different ionic states. Third, the IR spectrum of **1** showed absorption of carbonyls at 1661 and 1580 $cm^{-1}$, indicating the presence of an amide and carboxylate anion while the spectrum of **2** showed strong absorption of a carbonyl at 1673 $cm^{-1}$, indicating the presence of an amide and carboxylic acid. The working hypothesis of different ionic states was finally proven by protonation of **1** with 0.1N trifluoroacetic acid, followed by comparison of spectroscopic data (supplemental info).[14] The $^1H$ and $^{13}C$ data of protonated **1** are spectroscopically identical to those of **2**, and optical rotation values are similar. In addition, protonation of **1** changed chiroptical property of **1** and the CD absorption curve of protonated **1** is almost identical to that of **2** and semisynthetic **2**. Therefore, the proposed planar structure of **1** was amended to reflect its negatively charged state (Figure 1), and the HRESI $[M+H]^+$ *m/z* 743.3535 mass of **1** is likely the result of reduction during electrospray ionization.

To ascertain the absolute configuration of the Me-Cys residues, compound **1** was subjected to ozonolysis and oxidative workup prior to acid hydrolysis. The hydrolysate was analyzed by chiral HPLC and only D(*S*)-2-methylcysteic acid was detected.[15]

To determine the configuration of the remaining 10 stereocenters, semisynthetic hoiamide D, prepared by base hydrolysis of hoiamide A, was used for comparative analysis.[16] Semisynthetic hoiamide D was identical to **2** by LC-ESI-MS analyses (retention time, UV spectrum, and *m/z* value) and $^1H$ and $^{13}C$ NMR data analyses, had a similar optical rotation value and an identical CD spectrum to protonated **1** and **2** which indicated that natural hoiamide D (**1** and **2**) and semisynthetic hoiamide D were stereochemically identical (Figure 3b). The absolute configuration of natural hoiamide D (**1** and **2**) was thus determined as 2*R*, 3*S*, 4*S*, 5*S*, 11*S*, 15*R*, 23*S*, 24*R*, 25*R*, 26*S*, 27*S* and 28*R*.

The carboxylate anion (**1**) was screened in a panel of assays to determine its biological activity, and its greatest bioactivity was inhibition of p53/HDM2 (human homologue) interaction. A HTR-FRET-based competition assay was used to characterize antagonists of the p53/HDM2 binding interaction based on the ability of antagonist molecules to compete with biotin-labeled p53 protein (bio-QETFSDLWKLLP-Ac) binding to GST-tagged HDM2 (GST-MPRFMDYWEGLN).[17] FRET was detected (ex 320 nm, em 615, 665 nm) when donor labeled, Europium (Mab GST-Eu cryptate, Cisbio 61GSTKLB), and acceptor labeled,

XLent (streptavidin-XLent, Cisbio 611SAXLB), complexes were in close proximity due to the anti-GST/GST-HDM2 interaction and the streptavidin/biotin-p53 interaction. The carboxylate anion (**1**) inhibited the p53/HDM2 protein binding ($EC_{50}$= 4.5 μM; 95% confidence interval: 2.8-7.3 μM) with minimal cytotoxicity to the mammalian H460 cell line at 40 μM (16% ± 1), compared to control.[18] Compound **2** was not tested in the p53/HDM2 assay, although the carboxyl group would be deprotonated at the pH (7.4) of the media utilized in the assay.

Chlorofusin ($IC_{50}$= 4.6 μM), isolated from a marine fungus *Fusarium* sp., was the first natural product reported to inhibit p53/MDM2 interactions.[19] A second natural product inhibitor, the non-peptidic hexylitaconic acid ($IC_{50}$= 230 μM), was isolated from a marine fungus *Arthrinium* sp. in 2006, followed by sempervirine ($IC_{50}$= 29.4 μM).[20,21] Hoiamide D is the second peptide-based natural product inhibitor of p53/MDM2 interaction reported, and is one of the most potent. Of note, however, there are rationally designed synthetic inhibitors, such as the spiro-oxindoles and benzodiazepinediones, with nanomolar efficacy.

Hoiamide D joins three other hoiamides isolated to date, comprising a recently described class of cyanobacterial compounds featuring a triheterocylic system. Hoiamide A and B are cyclic whereas hoiamide C and D are linear.[22,23] In fact, hoiamide C may be an extraction artifact of hoiamide D given the utilization of ethanol in the storage conditions of the biological material. Hoiamide A and B exhibited potent inhibition of calcium oscillation in rat cortical neurons and micromolar activation of voltage-gated sodium channels (VGSC) with hoiamide A reported to be a partial agonist at site 2 of the mammalian VGSC.[23] Both hoiamide C and D were inactive in these assays, suggesting that a cyclic architecture is required for this potent neuromodulatory activity.[23] However, the activity of hoiamide D (**1**) in the p53/HDM2 assay suggests that this molecular class has the capacity to interact with a variety of cellular targets, and thus, members of this group should be attractive targets for total synthesis[24] and evaluation in a diversity of biological assays.

## Supplementary Material

Refer to Web version on PubMed Central for supplementary material.

## Acknowledgments

We thank the government of Papua New Guinea for permission to make these cyanobacterial collections, A. Pereira for the synthetic standard and technical expertise, T. Suyama for helpful advice, J. Wingerd and T. Byrum for the H-460 cytotoxicity and Neuro-2A screening, and the TSRI and UCSD mass spectrometry facilities for their analytical services. This work was supported by NIH grants CA 52955, NS 053398, and NIH/NCI CA100851.

## References and Notes

1. Mandinova A, Lee SW. Sci. Trans. Med. 2011; 3:64rv1.
2. Nigro JM, Baker SJ, Preisinger AC, Jessup JM, Hostetter R, Cleary K, Bigner SH, Davidson N, Baylin S, Devilee P, Glover T, Collins FS, Weslon A, Modali R, Harris CC, Vogelstein B. Nature. 1989; 342:705. [PubMed: 2531845]
3. Chene P. Mol. Cancer Res. 2004; 2:20. [PubMed: 14757842]
4. Kulikov R, Letienne J, Kaur M, Grossman SR, Arts J, Blattner C. Proc. Natl. Acad. Sci. U.S.A. 2010; 107:10038. [PubMed: 20479273]
5. Poyurovsky MV, Katz C, Laptenko O, Beckerman R, Lokshin M, Ahn J, Byeon IJ, Gabizon R, Mattia M, Zupnick A, Brown LM, Friedler A, Prives C. Nat. Struct. Mol. Biol. 2010; 17:982. [PubMed: 20639885]
6. Chene P. Nat. Rev. Cancer. 2003; 3:102. [PubMed: 12563309]
7. Dickens MP, Fitzgerald R, Fischer PM. Semin. Cancer Biol. 2010; 20:10. [PubMed: 19897042]

8. Patel S, Player MR. Expert Opin. Invest. Drugs. 2008; 17:1865.
9. Tidgewell, K.; Clark, BR.; Gerwick, WH. Comprehensive Natural Products Chemistry. Mander, L.; Lui, H-W., editors. Vol. 2. Elsevier; Oxford: 2010. p. 141-188.
10. Compound **1:** pale green solid; $[\alpha]_D$ −30 (*c* 0.05, MeCN); UV (MeCN) $\lambda_{max}$ (log ε) 252 (3.54); IR (neat) $\nu_{max}$ 3381, 2963, 2929, 1661, 1580, 1518, 1458, 1404, 1154, 1084, 1034, 1018 $cm^{-1}$; $^1H$ NMR (DMSO, 500 MHz) and $^{13}C$ NMR (DMSO, 75 MHz) data, see Table 1; (+)-HRESIMS $[M+H]^+$ *m/z* 743.3535 (calcd for $C_{35}H_{59}N_4O_7S_3$, 488.3546).
11. The collection (PNG-04-26-06-3) was extracted six times with heat using $CH_2Cl_2$:MeOH (2:1) and was further processed on silica gel using vacuum liquid chromatography with a 100% hexanes-EtOAc-MeOH gradient to generate nine subfractions A-I. Fraction I eluted with 100% MeOH and harbored the greatest p53/MDM2 inhibitory activity. Fraction I (259 mg) was subsequently filtered using a Waters RP C18 SPE cartridge with a MeOH gradient to yield four relatively pure subfractions. The most polar subfraction exhibited the greatest activity and was further examined.
12. Compound **(2):** pale yellow oil; $[\alpha]_D$ 19.6 (*c* 0.05, MeCN); UV (MeOH) $\lambda_{max}$ (log ε) 250 (3.49); IR (neat) $\nu_{max}$ 3378, 2965, 2930, 1674, 1521, 1458, 1382, 1299, 1203, 1139, 1088, 1026 $cm^{-1}$; $^1H$ NMR (DMSO, 500 MHz) and $^{13}C$ NMR (DMSO, 75 MHz) data, see Table 1; (+)-HRESIMS $[M+H]^+$ *m/z* 743.3535 (calcd for $C_{35}H_{59}N_4O_7S_3$, 488.3546).
13. The collection (PNG-12-16-03-4) was extracted repeatedly with $CH_2Cl_2$-MeOH (2:1) and further fractionated by silica gel vacuum column chromatography (VLC) to produce nine fractions (A-I). Fraction I was found to possess slight colon cancer selective inhibitory activity. This fraction was subjected to RP Sep-pak followed by RP HPLC [Phenomenex Hydro RP C18, 300 Å, 10 × 250 mm, 68% $CH_3CN/H_2O$ (0.001% trifluoroacetic acid) at 3 mL/min] to afford hoiamide D (2.4 mg).
14. Compound **1** (3.0 mg) was treated with 0.1N trifluoroacetic acid for 1 hr and dried under $N_2$.
15. A sample of **1** (2.1 mg) was dissolved in 3 mL of $CH_2Cl_2$ and treated with ozone at 25° C for 15 min. The sample was dried and further treated with 1 mL of $H_2O_2$-HCOOH (1:2) at 70° C for 30 min. l(*R*)-2-Methylcysteic acid (2.0 mg) and d(*S*)-2-methylcysteic acid (2.5 mg) standards were prepared and treated as above ( Pattenden G, Thom SM, Jones MF. Tetrahedron. 1993; 49:2131. ). The dry sample **1** was then hydrolyzed using 6N HCl (0.5 mL) for 2 hr at 110° C and analyzed by chiral HPLC [Phenomenex Chirex 3126 (D), 4.6 × 50 mm; 2 mM $CuSO_4$ in $H_2O$ at 0.3 mL/min; detection at 230 nm] to yield d(*S*)-2-methylcysteic acid with a retention time of 9.7 min (d-MeCysA $t_R$= 10.0 min; l-MeCysA $t_R$ = 12.0 min).[23]
16. A semi-synthetic standard of hoiamide D was prepared according to Choi H, Pereira AR, Cao Z, Shuman CF, Engene N, Byrum T, Matainaho T, Murray TF, Mangoni A, Gerwick WH. J Nat Prod. 2010; 73:1411. [PubMed: 20687534] $[\alpha]_D$ +25.2 (*c* 0.05, MeCN); UV (MeOH) $\lambda_{max}$ (log ε) 250 (3.52)
17. The FRET buffer used for all experiments was phosphate buffered saline (pH 7.4), 100 mM KF, 0.1% bovine serum albumin, and 5 mM ß-mercaptoethanol. Biotin-P53 (500 nM, final) was preincubated for 20 min with test compound (10-0.0781 μg/mL; 2-fold serial dilution), and a master mix was then added containing GST-HDM2 (2.5 nM, final), Mab GST-Eu cryptate (17 nM, final), and streptavidin XLent (9 nM, final); the solution was incubated for 1 hr. Data were collected in duplicate using the PerkinElmer EnVision 2103 Multilabel Reader using excitation filter 320nm, emission filters 665nM (to detect XLent) and 615 nM (to detect Europium), respectively, and the optical module Lance Eu/APC Dual 452. Percent inhibition compared to DMSO control was calculated for each concentration of test compound. Dose-response graph was generated using Graphpad Prism software (Graphpad Software Inc., San Diego, CA). The $EC_{50}$ values were determined by non-linear regression analysis using a logistic equation.
18. Alley MC, Scudiero DA, Monks A, Hursey ML, Czerwinski MJ, Fine DL, Abbott BJ, Mayo JG, Shoemaker RH, Boyd MR. Cancer Res. 1988; 48:589. [PubMed: 3335022]
19. Duncan SJ, Gruschow S, Williams DH, McNicholas C, Purewal R, Hajek M, Gerlitz M, Martin S, Wrigley SK, Moore M. J. Am. Chem. Soc. 2001; 123:554. [PubMed: 11456567]
20. Tsukamoto S, Yoshida T, Hosono H, Ohta T, Yokosawa H. Biorg. Med. Chem. Lett. 2006; 16:69.
21. Sasiela CA, Stewart DH, Kitagaki J, Safiran YJ, Yang Y, Weissman AM, Oberoi P, Davydov IV, Goncharova E, Beutler JA, Mcmahon JB, O'Keefe BR. J. Biomol. Screening. 2008; 13:229.
22. Pereira A, Cao Z, Murray TF, Gerwick WH. Chem. Biol. 2009; 16:893. [PubMed: 19716479]

23. Choi H, Pereira AR, Cao Z, Shuman CF, Engene N, Byrum T, Matainaho T, Murray TF, Mangoni A, Gerwick WH. J. Nat. Prod. 2010; 73:1411. [PubMed: 20687534]
24. Wang L, Xu Z, Ye T. Organic Lett. 2011; 13:2506.

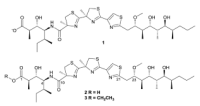

**Figure 1.**
Structures of the conjugate base of hoiamide D (**1**), the acid form of hoiamide D (**2**), and hoiamide C (**3**).

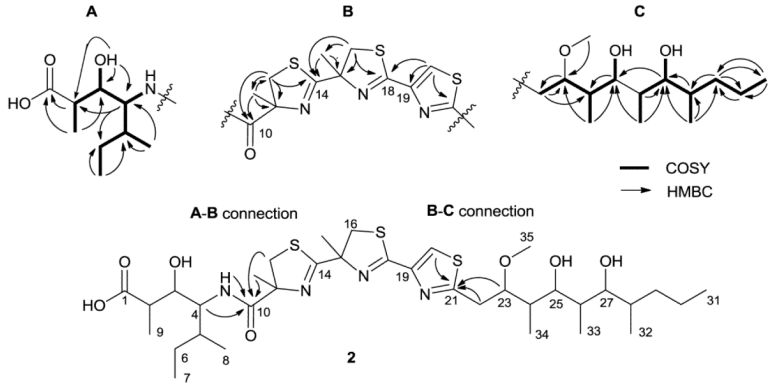


**Figure 2.**
Partial structures of **1** and **2** with key COSY and HMBC correlations.

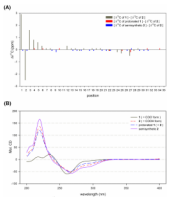

**Figure 3.**

Comparison of $^{13}C$ NMR chemical shifts and CD spectra of **1** (-$COO^-$ form), **2** (-COOH form), protonated **1** and semisynthetic **2** (**A**) $^{13}C$ NMR chemical shifts comparison; (**B**) CD absorption curve of **1** and **2** with protonated **1** and semisynthetic **2**.

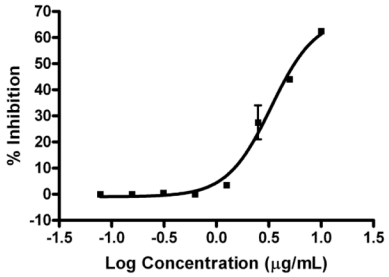


**Figure 4.**
Inhibition of p53/MDM2 binding by hoiamide D (**1**). $EC_{50}$= 4.5 μM; 95% confidence interval: 2.8-7.3 μM (n=2).

*Bioorg Med Chem Lett*. Author manuscript; available in PMC 2013 January 1.

**Table 1**

1H and 13C NMR data for the conjugate base (**1**) and acid (**2**) forms of hoiamide D (DMSO-*d*6).

| Position | Compound (1) | | | Compound (2) | | |
|---|---|---|---|---|---|---|
| | $\delta_H$ (J in Hz)[a] | $\delta_C$[b] | HMBC[a] | $\delta_H$ (J in Hz)[a] | dC[b] | HMBC[a] |
| 1 | | 179.5 | | | 176.5 | |
| 2 | 1.70, m | 41.6 | 9 | 2.17, dt (6.8, 10.9) | 44.1 | 1, 3, 9 |
| 3 | 3.51, d (10.8) | 71.8 | 1 | 3.81, m | 70.2 | 2 |
| 4 | 3.52, t (10.4) | 53.5 | 1, 5 | 3.53, d (9.6) | 52.7 | 2, 5, 6, 8, 10 |
| 5 | 1.61, m | 36.1 | | 1.58, m | 35.5 | 7 |
| 6a | 1.49, m | 25.4 | 3, 7 | 1.44, m | 25.1 | 7 |
| 6b | 1.04, m | | | 1.07, m | | 5, 7, 8 |
| 7 | 0.85, t (7.1) | 11.1 | 6 | 0.84, t (7.2) | 11.0 | 5, 6 |
| 8 | 0.88 d (6.8) | 15.7 | 4, 5 | 0.89, d (6.3) | 15.6 | 4, 5, 6 |
| 9 | 0.85, d (4.1) | 13.8 | 1, 2, 3 | 0.92, d (7.2) | 13.6 | 1, 2, 3 |
| NH | 6.85, d (9.7) | | 4, 10 | 6.93, d (9.8) | | 10 |
| 10 | | 173.3 | | | 173.3 | |
| 11 | | 84.4 | | | 84.4 | |
| 12a | 3.59, d (11.6) | 40.9 | 10, 11, 13, 14 | 3.61, d (11.3) | 40.6 | 10, 11, 13, 14 |
| 12b | 3.13, d (11.6) | | 10, 11, 13, 14 | 3.15, d (11.3) | | 10, 11, 13, 14 |
| 13 | 1.45, s | 25.7 | 10, 11, 12 | 1.44, s | 25.6 | 10, 11, 12 |
| 14 | | 177.7 | | | 177.6 | |
| 15 | | 83.6 | | | 83.7 | |
| 16a | 3.74, d (11.4) | 42.2 | 14, 15, 17, 18 | 3.78, d (11.1) | 42.1 | 14, 15, 17, 18 |
| 16b | 3.46, d (11.4) | | 14, 15, 17, 18 | 3.45, d (11.1) | | 14, 15, 17, 18 |
| 17 | 1.57, s | 26.0 | 14, 15, 16 | 1.62, s | 26.0 | 14, 15, 16 |
| 18 | | 162.5 | | | 162.4 | |
| 19 | | 146.4 | | | 146.5 | |
| 20 | 8.21, d (1.0) | 122.6 | 18, 19, 21 | 8.19, s | 122.5 | 18, 19, 21 |
| 21 | | 169.9 | | | 169.9 | |
| 22a | 3.17, m | 33.0 | 21 | 3.16, dd (3.7, 15.3) | 33.1 | 21, 23, 24 |
| 22b | 2.88, dd (10.5, 15.1) | | 21, 23 | 2.90, dd (11.0, 15.3) | | 21, 23, 24 |

| Position | Compound (1) | | | Compound (2) | | |
|---|---|---|---|---|---|---|
| | $\delta_H$ (J in Hz)[a] | $\delta_C$[b] | HMBC[a] | $\delta_H$ (J in Hz)[a] | dC[b] | HMBC[a] |
| 23 | 3.88, d (10.5) | 80.6 | 21 | 3.86, d (11.0) | 80.5 | 21, 22, 34, 35 |
| 24 | 2.08, m | 35.8 | 34 | 2.09, m | 35.9 | 34 |
| 25 | 3.75, d (10.4) | 69.4 | 24 | 3.74, d (10.0) | 69.7 | 24, 33 |
| 26 | 1.52, m | 37.3 | | 1.54, m | 37.3 | 27, 33 |
| 27 | 3.33, d (7.6) | 72.7 | 26 | 3.33, m | 73.1 | 25, 26, 32 |
| 28 | 1.54, m | 33.7 | 33 | 1.53, m | 33.8 | 27, 32 |
| 29a | 1.32, m | 36.7 | 28 | 1.31, m | 36.6 | 27, 28, 30, 31, 32 |
| 29b | 1.17, m | | 28, 30 | 1.18, m | | 27, 28, 30, 31, 32 |
| 30 | 1.30, m | 19.9 | | 1.30, m | 19.9 | 29, 31 |
| 31 | 0.85, t (7.1) | 14.3 | 30, 32 | 0.86, t (7.3) | 14.3 | 29, 30 |
| 32 | 0.75, d(6.4) | 12.8 | 27, 28 | 0.76, d (6.6) | 12.8 | 28, 29 |
| 33 | 0.71, d (7.1) | 9.0 | 25, 26, 27 | 0.71, d (6.7) | 9.0 | 25, 26, 27 |
| 34 | 0.72, d (7.5) | 9.6 | 23, 24, 25 | 0.73, d (6.6) | 9.6 | 23, 25 |
| 35 | 3.22, s | 56.2 | 23 | 3.21, s | 56.2 | 23 |
| 1-OH | | | | 12.0, s | | |
| 3-OH | 5.32 brs | | | 5.29, d (4.7) | | 2, 3, 4 |
| 26-OH | 4.50, s | | | 4.27, s | | |
| 27-OH | | | | 4.23, s | | |

[a] 500 and 600 MHz for $^1$H NMR, HMBC

[b] 75 MHz for $^{13}$C NMR